
Deep Mixture of Experts via Shallow Embedding

Xin Wang¹ Fisher Yu¹ Ruth Wang¹ Yi-An Ma¹ Azalia Mirhoseini²
Trevor Darrell¹ Joseph E. Gonzalez¹

¹EECS Department, UC Berkeley ²Google Brain

Abstract

Larger networks generally have greater representational power at the cost of increased computational complexity. Sparsifying such networks has been an active area of research but has been generally limited to static regularization or dynamic approaches using reinforcement learning. We explore a mixture of experts (MoE) approach to deep dynamic routing, which activates certain experts in the network on a per-example basis. Our novel DeepMoE architecture increases the representational power of standard convolutional networks by adaptively sparsifying and recalibrating channel-wise features in each convolutional layer. We employ a multi-headed sparse gating network to determine the selection and scaling of channels for each input, leveraging exponential combinations of experts within a single convolutional network. Our proposed architecture is evaluated on several benchmark datasets and tasks, and we show that DeepMoEs are able to achieve higher accuracy with lower computation than standard convolutional networks.

1 Introduction

Increasing network depth has been a dominant trend [11] in the design of deep neural networks for computer vision. However, increased network depth comes at the expense of computational overhead and increased training time. To reduce the computational cost of machine translation models, Shazeer et al. [21] recently explored the design of “outrageously” wide sparsely-gated mixture of experts models. They demonstrated that these relatively shallow models can reduce computational costs and improve prediction accuracy. However, their resulting models needed to be many times larger than existing translation models to recover state-of-the-art translation accuracy. Preliminary work by Eigen et al. [9] demonstrated the advantages of stacking *two* layers of mixture of experts models for MNIST digits classification. A natural question arises: *can we stack and train many layers of mixture of experts models to improve accuracy and reduce prediction cost without radically increasing the network width?*

In this paper, we explore the design of *deep mixture of experts models (DeepMoEs)* that compose hundreds of mixture of experts layers. DeepMoEs combines the improved accuracy of deep models with the computational efficiency of sparsely-gated mixture of expert models. In addition, the composition of multiple sparsely-gated expert selection layers yields a potentially exponential increase in the representation capacity with only a linear increase in the number of parameters.

However, constructing and training DeepMoEs requires addressing several key challenges. First, mixture decisions interact across layers in the network requiring joint reasoning and optimization. Second, the discrete expert selection process is non-differentiable complicating gradient-based training. Finally, the composition of multiple mixture of experts models increases the chance of degenerate (i.e., singular) combinations of experts at each layer.

To address these challenges we propose a general DeepMoE architecture that combines a deep convolutional network with a shallow embedding network and a multi-headed sparse gating network. The shallow embedding network terminates in a soft-max output layer that computes *latent mixture*

weights over a fixed set of latent experts. These latent mixture weights are then inputted to the multi-headed sparse gating networks (with ReLU outputs) to select and *re-weight* the channels in each layer of the base convolutional network. We then jointly train the base model, shallow embedding network, and multi-headed gating network using a differentiable loss function which encourages diversity in the latent mixture weights and sparsity in the layer selection.

By stacking multiple mixture of experts layers, DeepMoE is able to achieve a substantial increase in representational capacity over a single wide mixture of experts layer. To characterize this increase in representational capacity, we analyze the combinatorial path structure and show that the expressive power is exponential in the depth of the network.

DeepMoE can be configured to increase accuracy and reduce computation costs. When used with wider convolutional networks (i.e., *wide-DeepMoE*), DeepMoE improves prediction accuracy without increasing the computation cost. Alternatively, combined with more typical narrow convolutional networks (i.e., *narrow-DeepMoE*), DeepMoE substantially reduces prediction costs without significantly impacting accuracy. In the later setting, DeepMoE generalizes existing work [18] on dynamic channel pruning and produces models that are both more accurate and more efficient.

Finally, we empirically evaluate the DeepMoE architecture on both image classification and semantic segmentation tasks using several benchmark datasets (i.e., CIFAR-10, CIFAR-100, ImageNet2012, CityScapes) where DeepMoE is able to achieve higher accuracy with lower computation. In particular, wide-DeepMoE improves the ResNet accuracy over 1% on ImageNet on which the latest shallow MoE work [10] failed to show any improvement. In addition, narrow-DeepMoE can be both more accurate and efficient than a range of dynamic and static channel pruning techniques and even improve the prediction accuracy over the baselines. We also conduct extensive ablation studies to understand the gating behaviors of DeepMoEs and investigate the design choices of DeepMoEs.

2 Related Work

Mixture of experts. Jacobs et al. [14] introduced the original formulation of mixture of experts (MoE) models. In this early work, they describe a learning procedure for systems composed of many separate neural networks each devoted to subsets of the training data. Later work [6, 7, 15] applied the MoE idea to classic machine learning algorithms such as support vector machines. More recently, several [21, 10, 1] have proposed MoE variants for deep learning in language modeling and image recognition domains. These more recent efforts to combine deep learning and mixtures of experts have focused on mixtures of deep sub-networks rather than stacking many mixture of expert models. While preliminary work by Eigen et al. [9] explored stacked MoE models, they only successfully demonstrated networks up to depth two and only evaluated their design on MNIST Digits. In this work, we construct deep models with hundreds of MoE layers based on a shared shallow embedding rather than the layer outputs [9] which makes DeepMoE more suitable to parallel hardware with batch parallelism as the gate decisions are pre-determined. We also address several of the key challenges around the design and training of multi-layer MoE models.

Conditional computation. Related to mixture of experts, recent work by Bengio et al. [2, 3, 4] explored conditional computation in the context of neural networks which selectively executes part of the network based on the input. They use reinforcement learning (RL) for the discrete selection decisions which are very delicate to train while our sparsely-gated MoE design can be embedded into standard convolutional networks and optimized with stochastic gradient descent.

Dynamic channel pruning. To reduce storage and computation overhead, many [17, 12, 19] have explored channel level pruning which removes entire channels at each layer in the network and thus leads to structured sparsity. However, permanently dropping channels limits the network capacity. Bridging conditional computation and channel pruning, recent works [18, 24] have explored dynamic pruning. Dynamic pruning uses per-layer gating networks to dynamically drop individual channels or entire layers based on the output of previous layers. Like the work on conditional computation, dynamic pruning relies on sample inefficient reinforcement learning techniques to train many convolutional gates. In this work, we generalize the earlier work on dynamic channel pruning by introducing a more efficient shared convolutional embedding and simple ReLU based gates to enable sparsification and feature re-calibration and allowing end-to-end training using stochastic gradient based methods.

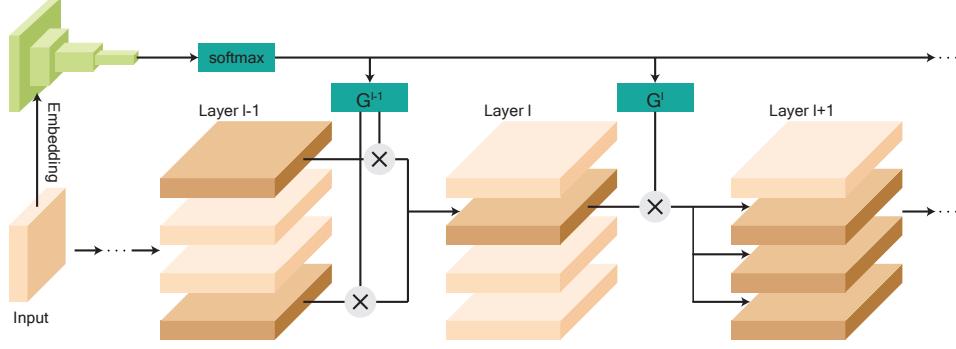


Figure 1: Deep Mixture of Experts via Shallow Embedding

3 Deep Mixture of Experts

The original mixture of experts [14] formulation combines a set of experts (classifiers), E_1, \dots, E_C , using a mixture (gating) function G that returns a distribution over the experts given the input \mathbf{x} :

$$y = \sum_{i=1}^C G(\mathbf{x})_i E_i(\mathbf{x}). \quad (1)$$

Here $G(\mathbf{x})_i$ is the weight assigned to the i^{th} expert E_i . Later work [7] generalized this mixture of experts formulation to a non-probabilistic setting where the gating function G outputs arbitrary weights for the experts instead of probabilities. We adopt this non-probabilistic view since it provides increased flexibility in re-scaling and composing the expert outputs.

3.1 Deep Mixture of Experts via Shallow Embedding

In this work, we propose the DeepMoE architecture which extends the standard single-layer MoE model to multiple layers within a single convolutional network. The experts in each MoE layer consist of the output channels of the previous convolution operation. In this section, we derive the equivalence between gated channels in a convolution layer and the classic mixture of experts formulation.

A convolution layer with tensor input \mathbf{x} having spatial resolution $W \times H$ and C^{in} input channels, and $C^{\text{in}} \times k \times k \times C^{\text{out}}$ convolutional kernel \mathbf{K} can be written as:

$$\mathbf{z}_{o,s,t} = \sum_{i=1}^{C^{\text{in}}} \sum_{u=0}^{k-1} \sum_{v=0}^{k-1} \mathbf{K}_{i,u,v,o} \mathbf{x}_{i,s+u,t+v}, \quad (2)$$

where \mathbf{z} is the $C^{\text{out}} \times W \times H$ output tensor. To construct an MoE convolutional layer we scale the input channels by the gate values $\mathbf{g} \in \mathbb{R}^{C^{\text{in}}}$ for that layer and rearrange terms:

$$\mathbf{z}_{o,s,t} = \sum_{i=1}^{C^{\text{in}}} \sum_{u=0}^{k-1} \sum_{v=0}^{k-1} \mathbf{g}_i \mathbf{K}_{i,u,v,o} \mathbf{x}_{i,s+u,t+v} = \sum_{i=1}^{C^{\text{in}}} \mathbf{g}_i \left(\sum_{u=0}^{k-1} \sum_{v=0}^{k-1} \mathbf{K}_{i,u,v,o} \mathbf{x}_{i,s+u,t+v} \right), \quad (3)$$

Defining convolution operator $*$, we can eliminate the summations and subscripts in (3) to obtain:

$$\mathbf{z} = \sum_{i=1}^{C^{\text{in}}} \mathbf{g}_i \mathbf{K}_i * \mathbf{x}_i = \sum_{i=1}^{C^{\text{in}}} \mathbf{g}_i E_i(\mathbf{x}). \quad (4)$$

Thus, we have shown that gating the input channels to a convolutional network is equivalent to constructing a mixture of experts for each output channel. In the following, we first describe how the gate values \mathbf{g} are obtained for each layer and then present how individual mixture of experts (channels) layers can be efficiently composed and trained in the DeepMoE architecture.

3.2 The DeepMoE Architecture

DeepMoE is composed of a base convolutional network, a shallow embedding network, and a multi-headed sparse gating network. The base convolutional network is a deep network where each convolution layer is replaced with an MoE convolution layer as described above. In our experiments we use ResNet [11], VGG [22] and DLA [27] as the base convolutional network architecture.

The mixture weights for each MoE convolutional layer are determined using the shallow embedding network and the multi-headed sparse gating network. The shallow embedding maps the raw input image into latent mixture weights. To reduce the computational overhead of the embedding network, we use a 4-layer (for CIFAR) or 5-layer (for ImageNet) convolutional network with 3-by-3 filters with stride 2 (roughly 2% of the computation of the base models). The multi-headed sparse gating network transforms the latent mixture weights produced by the shallow embedding network into sparse mixture weights for each layer in the convolutional network. The gate for layer l is defined as:

$$G^l(\mathbf{e}) = \text{ReLU}(W_g^l \cdot \mathbf{e}), \quad (5)$$

where \mathbf{e} is the output of the shared embedding network Emb and W_g^l are the learned parameters which, using the ReLU, project the latent mixture weights into *sparse* layer specific gates.

We refer to this gating design as *on demand gating*. The number of experts chosen at each level is data-dependent and the expert selection across different layers can be optimized jointly. Unlike the “noisy Top-K” design in [21], it is not necessary to determine the number of experts at each layer and indeed each layer can learn to use a different number of experts.

3.3 Loss Formulation and End-to-end Training

As with standard convolutional neural networks, DeepMoE models can be trained end-to-end using gradient based methods. The overall goals of the DeepMoE are twofold: to achieve high prediction accuracy and to learn a gating policy that selects a low-cost mixture of experts for each input. To this end, given the input \mathbf{x} and the target y , we define the learning objective as

$$\mathcal{J}(\mathbf{x}; y) = \mathcal{L}_b(\mathbf{x}; y) + \lambda \mathcal{L}_g(\mathbf{x}) + \mu \mathcal{L}_e(\mathbf{x}; y), \quad (6)$$

where \mathcal{L}_b is the cross entropy loss for the base convolutional model. The \mathcal{L}_g term defined:

$$\mathcal{L}_g(\mathbf{x}) = \sum_{l=1}^L \|G^l(Emb(\mathbf{x}))\|_1, \quad (7)$$

is used to control the computational cost (via the λ parameter) by encouraging sparsity in the gating network. Finally, we introduce an additional embedding classification loss \mathcal{L}_e to help balance utilization across the latent experts and mitigate the tendency towards degenerate expert combinations. This later loss encourages the embedding or some transformation of the embedding to also be predictive of the class label.

Because the DeepMoE loss is differentiable we train all three sub-networks jointly using stochastic gradient descent. Once trained, we then set λ and μ to 0 and continue to train a few more epochs to refine the base convolutional network. The full training algorithm is described in Procedure 1.

Procedure 1 Training Algorithm for DeepMoE

```

1: repeat
2:    $e \leftarrow \text{EmbeddingNetwork}(x)$ 
3:   for  $i$  from 1 to  $L$  do
4:      $g^i \leftarrow G^i(e)$ 
5:   end for
6:    $output \leftarrow \text{BaseNetwork}(x, g^1, \dots, g^L)$ 
7:    $\mathcal{L}_b \leftarrow \text{CrossEntropy}(output, y) + \lambda \sum_{l=1}^L \|g^l\|_1 + \mu \text{CrossEntropy}(e, y)$ 
8:   Optimize  $\mathcal{L}_b$  with SGD
9: until The model has been trained for  $n_0$  epochs
10: Freeze EmbeddingNetwork and  $G^l$  for  $l = 1, \dots, L$ ,  $\lambda \leftarrow 0$ ,  $\mu \leftarrow 0$ 
11: Repeat the training loop for another  $n_1$  epochs

```

4 Expressive Power of *Wide* DeepMoE

One way to increase the expressive power of a convolutional neural network is to increase the number of channels in the convolutional layers. However, the computational cost also increases as the network becomes *wider*. To address the trade-off between expressive power and computational cost, we show that the expressive power of DeepMoE increases exponentially with the number of layers. We outline the theoretical analysis in this section and provide details in the appendix (Sec.A.1).

We define the expressive power of DeepMoE to be the ability to construct arbitrary labeling for all possible distinct input values. Following [5], we view a neural network as a mapping from a particular example to a cost function (e.g., the log probability) over labels for that example. To be able to map different data to different values of the cost function, we combine and concatenate simple convolution units together. We show that the bottleneck of a network’s expressive power is the number of possible combinations of these convolution units. We demonstrate in Sec.A.1 that increasing the depth of the network results in a doubly exponential increase in the possible combinations of mappings based on network width. While sparsity could reduce the possible combinations, we also show there that given sufficient diversity in the sparsity, the probability that the sparsity reduces the effective number of combinations decreases exponentially in the network depth.

5 Experiments

We evaluate both wide-DeepMoE and narrow-DeepMoE on the image classification and semantic segmentation tasks. For image classification task we use the CIFAR-10 [16], CIFAR-100 [16] and ImageNet 2012 benchmark datasets [20] (Sec. 5.1 and 5.2). For the semantic segmentation task we use the CityScapes [8] dataset (in the Sec. A.2). We apply standard data augmentation using basic mirroring and shifting [23] for CIFAR datasets and scale and aspect ratio augmentation with color perturbation [25] for ImageNet. We also conduct ablation studies in Sec. 5.3- 5.5.

Models. We examine DeepMoE with a wide range of network designs: VGG network [22], ResNet [11] and DLA [27]. VGG is a typical feed-forward convolutional network without skip connections and feature aggregation while the other two which compose of many residual blocks have more complicated connections. To construct DeepMoE, we need to add a gating header after each convolutional layer in VGG and modify the residual blocks as shown in Fig. 2. In wide-DeepMoE, we increase the number of channels in each convolutional layer by a factor of two unless stated otherwise. In narrow-DeepMoE, we retain the same channel configuration as the original base convolutional model. All the models are implemented in PyTorch, and the code will be open-sourced.

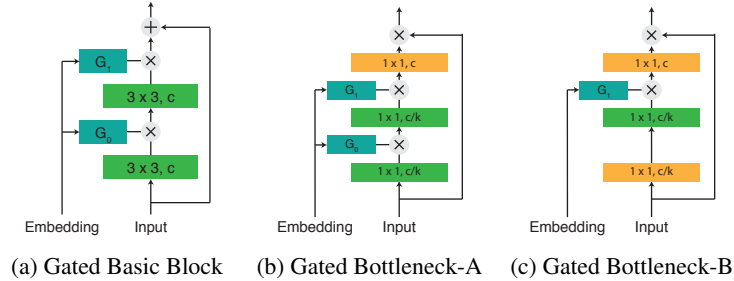
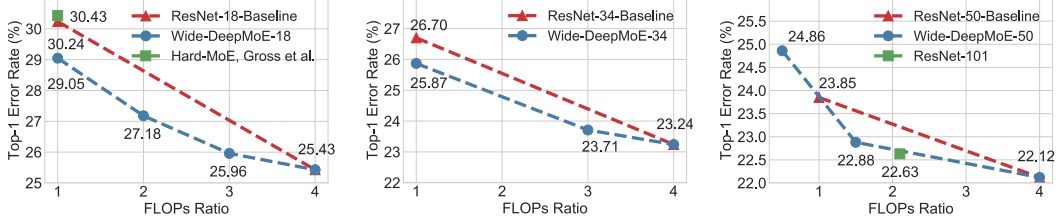


Figure 2: Gated Residual Block Designs. The bottleneck-A and B are used in ResNet-50 on ImageNet and the basic block for in all the other models. In wide-DeepMoE, we increase the number of channels of layers in green

Training. To train DeepMoE we follow common training practices [11, 27]. For the CIFAR datasets, we start training with learning rate 0.1 for ResNet and 0.01 for VGG16, which is reduced by $10\times$ at 150 and 250 epochs with total 350 epochs for the baselines and 270 epochs for DeepMoE joint optimization stage and another 80 epochs for fine-tuning with fixed gating networks. For ImageNet, we train the network with initial learning rate 0.1 for 100 epochs and reduce it by $10\times$ every 30 epochs. We do not further fine-tune the base convolutional network on ImageNet as we find the improvement from fine-tuning is marginal compared to that on CIFAR datasets. We set the computational cost parameter λ in the DeepMoE loss function (Eq. 6) between $[0.001, 8]$ (larger values reduce computation). We set $\mu = 1$ for the CIFAR datasets to match the scale of the cross entropy loss on the base model. For ImageNet we set $\mu = 0$ to improve base model feature extraction.

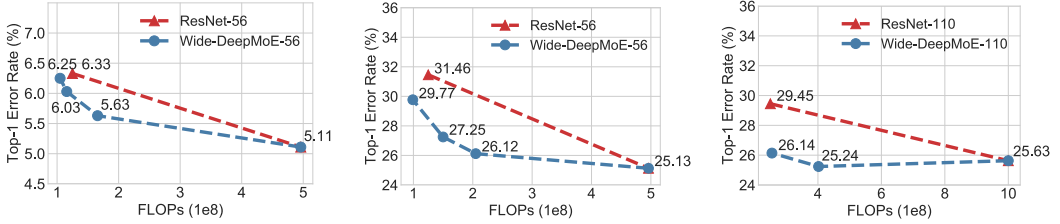
5.1 Wide-DeepMoE: Improved Accuracy with Reduced Computation

In this section, we study how increasing model capacity affects the prediction accuracy of the models. We evaluate ResNet-56 and ResNet-110 on the CIFAR-10 and CIFAR-100 datasets and ResNet-18, 34 with the basic block (Fig. 2a) and 50 with the bottleneck-A (Fig. 2b) on ImageNet. We show the accuracy and computation cost measured by FLOPs (multiply-adds) trade-off curves on the ImageNet (Fig. 3) and the CIFAR-10 and CIFAR-100 (Fig. 4). The FLOPs ratio in Fig. 3 is the relative computation ratio to the baseline convolutional network. For example, because computation scales quadratically with the number of channels, the FLOPs ratio of a model with twice the number of channels would be $4\times$ compared to the baseline model.



(a) wide-DeepMoE with ResNet-18 (b) wide-DeepMoE with ResNet-34 (c) wide-DeepMoE with ResNet-50

Figure 3: (a) and (b) wide-DeepMoE improves the accuracy on ImageNet by $\sim 1\%$. (c) wide-DeepMoE with ResNet-50 reduces 20% FLOPs of ResNet-101 with a 0.2% difference in accuracy



(a) 56-layer Model on CIFAR-10 (b) 56-layer Model on CIFAR-100 (c) 110-layer Model on CIFAR-100

Figure 4: Wide-DeepMoE with ResNet-56 and ResNet-100 on CIFAR datasets. Wide-DeepMoE improves the prediction accuracy of the baseline ResNet by 3~4% on CIFAR-100

As we can see from Fig. 3 and Fig. 4, wide-DeepMoE achieves lower prediction error with lower or comparable computation when compared to standard ResNet models. In particular, wide-DeepMoE with ResNet-18 and 34 reduce $\sim 1\%$ Top-1 error on ImageNet on which the previous work [10] fails to show any improvement. We also note that Wide-DeepMoE with ResNet-50 achieves 22.88% top-1 error rate which is only 0.2% lower than ResNet-101 with 20% less computation. Similar results can be observed on CIFAR datasets though the improvement on CIFAR-10 is relatively small (0.3) since the opportunity gap between DeepMoE and the standard ResNet is small (1.2%).

We also examine memory usage and find that wide-DeepMoE with ResNet-50 using Bottleneck-B (Fig. 2c), which is more memory efficient than Bottleneck-A (Fig. 2b), achieves 22.84% top-1 error with 6% less parameters and 18% less FLOPs, indicating that wide-DeepMoE is competitive on the memory usage even though it is not the main optimization goal of DeepMoE.

5.2 Narrow-DeepMoE vs (Dynamic) Channel Pruning

DeepMoE generalizes existing channel pruning work since it both dynamically prunes and *re-scales* channels to reduce the computational cost and improve accuracy. In previous dynamic channel pruning work, channels are pruned based on the outputs of previous layers. In contrast, the gate decisions in DeepMoEs are determined in advance based on the shared embedding (latent mixture weights) which enables improved batch parallelism at inference.

We compare DeepMoE to the latest dynamic channel pruning work RNP [18] with VGG-16¹ as the base model on CIFAR-100. As we can see from Fig. 5a, without fine-tuning, the prediction error and computation trade-off curve (dotted blue line) of DeepMoE is much flatter than RNP (dotted red line) which indicates DeepMoE has a greater reduction in computation without loss of accuracy. Moreover, when fine-tuning DeepMoE for only 10 epochs (dotted green line in Fig. 5a), DeepMoE improves the prediction accuracy by a large margin by 4% which is a $\sim 13\%$ improvement over the baseline VGG model due to the regularization effect of DeepMoE (Sec. 5.5).

In addition, DeepMoE outperforms the state-of-the-art static channel pruning results [19, 11, 17, 13] on both ImageNet and CIFAR-10. DeepMoE with ResNet-50 reduces 56.8% of the computation of the standard ResNet-50 with a top-1 error rate of 26.21%, approximately 2% better than [12], which currently has the best accuracy for an equivalent amount of computation among previous work on ImageNet. Details are in Tab. 1 and Fig. 5.

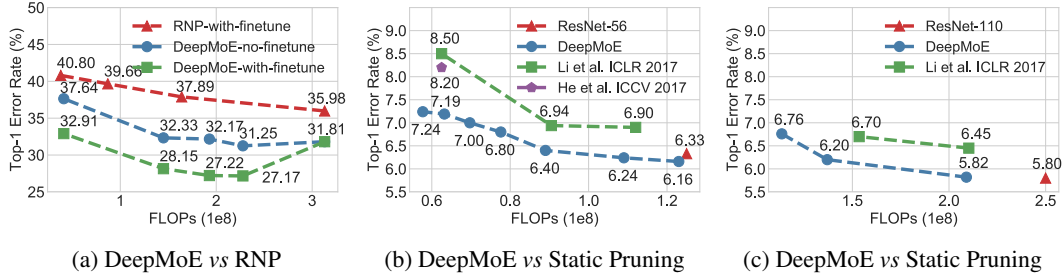


Figure 5: (a) DeepMoE vs the dynamic pruning approach RNP on CIFAR-100 with VGG16. DeepMoE not only outperforms RNP on the accuracy-computation trade-off but improves the accuracy over the baseline VGG model. (b) and (c) DeepMoE vs static pruning approaches on CIFAR-10

Model	Top-1 Error	Top-5 Error	FLOPs (x10 ⁹)	Reduction (%)
ResNet-18	30.24	10.92	1.80	-
DeepMoE-DLA-34-v1	30.412	10.91	0.79	74.32
Pruned ResNet-50 ThiNet [19]	28.99	9.98	1.68	55.8
Pruned ResNet-50 He et al. [12]	-	9.20	1.90	50.0
DeepMoE-DLA-34-v2	28.22	9.42	1.69	44.78
DeepMoE-ResNet-50	26.21	8.42	1.64	56.81
Pruned ResNet-50 Huang et al. [13]	26.80	-	3.03	20.26
Pruned ResNet-50 Li et al. [17]	27.02	8.92	3.08	18.95

Table 1: DeepMoE vs static pruning on ImageNet. DeepMoE-ResNet-50 wins on both accuracy and computation. DeepMoE-DLA-34-v1 ($\lambda = 4$) has less than half of the computation of ResNet-18 with similar accuracy

5.3 Gating Behavior Analysis

To analyze the gating behavior of DeepMoE, we evaluate the trained DeepMoE with VGG-16 as follows: for a given fine-grained class A (e.g., *dolphin*), we re-assign the gate embedding for each input in class A with a randomly chosen gate embedding from other classes either within the same coarse category (referred to as *in-group shuffling*) or different categories (referred to as *out-of-group shuffling*). In Fig. 6a, we plot the test accuracy of class *dolphin*, belonging to the coarse category *aquatic mammals* with randomly selected gate embeddings (repeated 20 times for each input) from classes in the same coarse category (in red) and 5 classes for other coarse categories (in blue). The test accuracy with in-group shuffling is much higher than that with out-of-group shuffling. Especially when applying the gate embeddings from the tulip category, the test accuracy drops to 1% while the accuracy with in-group shuffling is mostly above 50%. This indicates that the latent mixture weights are similar for semantically related image categories. This result is significant given DeepMoE is never given this coarse class structure.

¹Our baseline accuracy is higher than RNP since we use a version with batch normalization in contrast to the published method.

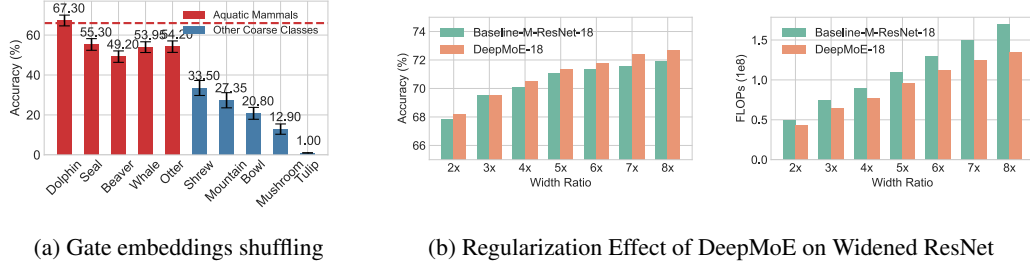


Figure 6: (a) Gate embedding shuffling. The in-group shuffling has much higher accuracy than the out-of-group shuffling. (b) wide-DeepMoE is both more accurate and efficient than the widened baseline models

5.4 DeepMoE vs Single-Layer MoE

So far in our experiments, we have widened the network by increasing the number of channels for all convolutional layers. Here, we study other strategies for widening the network. We, therefore, try widening the VGG-16 model in four different ways: widen the top layer (W1-High), widen the middle layer (W1-Mid), widen the lower 4 layers (W4-Low), and finally widen all the 13 convolutional layers (W13-All) as used in all the other experiments (details in Sec. A.4).

Control	Model	# Params	FLOPs ($\times 10^8$)	Accuracy (%)
# Params	W1-High	24.15M	3.51	71.96
	W1-Mid	24.16M	9.18	72.02
	W4-Low	24.18M	43.16	72.51
	W13-All	24.18M	8.15	73.91
# Params and FLOPs	W1-High	24.15M	2.98	73.28
	W1-Mid	24.16M	2.74	72.68
	W4-Low	24.18M	2.45	73.33
	W13-All	24.18M	2.29	73.39

Table 2: Different widening strategies for VGG16 on CIFAR-100

Shown in Tab. 2, with the same number of parameters, the prediction accuracy of W13-All is strictly better than that of a single-layer MoE. Adding MoE to the bottom or top layers is more effective than adding it to the middle layer. Alternatively, if we control both the number of parameters and the computation FLOPs, the accuracy differences between different strategies are reduced but W13-All is still more favorable to a single-layer MoE.

5.5 Regularization Effect of DeepMoE

Since DeepMoE sparsifies the channel outputs during training and testing, we study the regularization effect of such sparsification. We increase the number of channels of a modified ResNet-18 with bottleneck-B (in Fig. 2c) by $2-8\times$ on CIFAR-100. We show the accuracy and the computation FLOPs of the baseline widened ResNet-18 models and wide-DeepMoE with $\lambda = 2$ in Fig. 6b. Wide-DeepMoE has a lower computation cost and is also more accurate than the baseline wide convolutional network. Furthermore, the advantage of DeepMoE increases with the width of the base convolutional network suggesting a potential regularizing effect to the DeepMoE design.

6 Conclusion

In this work, we explored the design of deep mixture of experts models for computer vision applications. We developed a novel DeepMoE architecture that leverages a shallow embedding network to construct latent mixture weights. We then used sparse multi-headed gating networks to select and re-weight individual channels at each layer in the deep convolutional network. This design in conjunction with a novel sparsifying and diversifying loss enabled joint differentiable training addressing the key limitations of existing mixture of experts approaches in deep learning. We demonstrated that DeepMoE is able to reduce computation and improve accuracy over baseline convolutional networks. On the challenging ImageNet benchmark we improved upon the state-of-the-art residual network result by a full 1%. We also studied the behavior of the latent mixture weights and found that they are able to resolve coarse grain class structure in the underlying problem.

References

- [1] K. Ahmed, M. H. Baig, and L. Torresani. Network of experts for large-scale image categorization. In *European Conference on Computer Vision*, pages 516–532. Springer, 2016.
- [2] E. Bengio, P.-L. Bacon, J. Pineau, and D. Precup. Conditional computation in neural networks for faster models. *arXiv preprint arXiv:1511.06297*, 2015.
- [3] Y. Bengio, N. Léonard, and A. Courville. Estimating or propagating gradients through stochastic neurons for conditional computation. *arXiv preprint arXiv:1308.3432*, 2013.
- [4] K. Cho and Y. Bengio. Exponentially increasing the capacity-to-computation ratio for conditional computation in deep learning. *arXiv preprint arXiv:1406.7362*, 2014.
- [5] N. Cohen, O. Sharir, and A. Shashua. On the expressive power of deep learning: A tensor analysis. In *Conference on Learning Theory*, pages 698–728, 2016.
- [6] R. Collobert, S. Bengio, and Y. Bengio. A parallel mixture of svms for very large scale problems. In *Advances in Neural Information Processing Systems*, pages 633–640, 2002.
- [7] R. Collobert, Y. Bengio, and S. Bengio. Scaling large learning problems with hard parallel mixtures. *International Journal of pattern recognition and artificial intelligence*, 17(03):349–365, 2003.
- [8] M. Cordts, M. Omran, S. Ramos, T. Rehfeld, M. Enzweiler, R. Benenson, U. Franke, S. Roth, and B. Schiele. The cityscapes dataset for semantic urban scene understanding. In *Proc. of the IEEE Conference on Computer Vision and Pattern Recognition (CVPR)*, 2016.
- [9] D. Eigen, M. Ranzato, and I. Sutskever. Learning factored representations in a deep mixture of experts. *International Conference on Learning Representations Workshop*, 2014.
- [10] S. Gross, M. Ranzato, and A. Szlam. Hard mixtures of experts for large scale weakly supervised vision. In *Proceedings of the IEEE Conference on Computer Vision and Pattern Recognition*, pages 6865–6873, 2017.
- [11] K. He, X. Zhang, S. Ren, and J. Sun. Deep residual learning for image recognition. In *Proceedings of the IEEE conference on computer vision and pattern recognition*, pages 770–778, 2016.
- [12] Y. He, X. Zhang, and J. Sun. Channel pruning for accelerating very deep neural networks. In *International Conference on Computer Vision (ICCV)*, volume 2, page 6, 2017.
- [13] Z. Huang and N. Wang. Data-driven sparse structure selection for deep neural networks. *arXiv preprint arXiv:1707.01213*, 2017.
- [14] R. A. Jacobs, M. I. Jordan, S. J. Nowlan, and G. E. Hinton. Adaptive mixtures of local experts. *Neural computation*, 3(1):79–87, 1991.
- [15] M. I. Jordan and R. A. Jacobs. Hierarchical mixtures of experts and the EM algorithm. *Neural computation*, 6(2):181–214, 1994.
- [16] A. Krizhevsky and G. Hinton. Learning multiple layers of features from tiny images. 2009.
- [17] H. Li, A. Kadav, I. Durdanovic, H. Samet, and H. P. Graf. Pruning filters for efficient convnets. *International Conference on Learning Representations*, 2017.
- [18] J. Lin, Y. Rao, J. Lu, and J. Zhou. Runtime neural pruning. In *Advances in Neural Information Processing Systems*, pages 2178–2188, 2017.
- [19] J.-H. Luo, J. Wu, and W. Lin. ThiNet: A filter level pruning method for deep neural network compression. In *Proceedings of the IEEE Conference on Computer Vision and Pattern Recognition*, pages 5058–5066, 2017.
- [20] O. Russakovsky, J. Deng, H. Su, J. Krause, S. Satheesh, S. Ma, Z. Huang, A. Karpathy, A. Khosla, M. Bernstein, et al. Imagenet large scale visual recognition challenge. *International Journal of Computer Vision*, 115(3):211–252, 2015.

- [21] N. Shazeer, A. Mirhoseini, K. Maziarz, A. Davis, Q. Le, G. Hinton, and J. Dean. Outrageously large neural networks: The sparsely-gated mixture-of-experts layer. *International Conference on Learning Representations*, 2017.
- [22] K. Simonyan and A. Zisserman. Very deep convolutional networks for large-scale image recognition. *arXiv preprint arXiv:1409.1556*, 2014.
- [23] L. Wan, M. Zeiler, S. Zhang, Y. Le Cun, and R. Fergus. Regularization of neural networks using dropconnect. In *International Conference on Machine Learning*, pages 1058–1066, 2013.
- [24] X. Wang, F. Yu, Z.-Y. Dou, and J. E. Gonzalez. SkipNet: Learning dynamic routing in convolutional networks. *arXiv preprint arXiv:1711.09485*, 2017.
- [25] S. Xie, R. Girshick, P. Dollár, Z. Tu, and K. He. Aggregated residual transformations for deep neural networks. In *Computer Vision and Pattern Recognition (CVPR), 2017 IEEE Conference on*, pages 5987–5995. IEEE, 2017.
- [26] F. Yu, V. Koltun, and T. Funkhouser. Dilated residual networks. In *Computer Vision and Pattern Recognition*, volume 1, 2017.
- [27] F. Yu, D. Wang, and T. Darrell. Deep layer aggregation. *Proceedings of the IEEE conference on computer vision and pattern recognition*, 2018.

Appendix

A.1 Expressive Power of *Wide* DeepMoE

To characterize the expressive power of DeepMoE, we follow the tensor analysis approach of Cohen et al. [5]. We first represent an instance of data as a collection of vectors $(\mathbf{x}_1, \dots, \mathbf{x}_N)$, where $\mathbf{x}_i \in \mathbb{R}^s$. For the image data, the collection $(\mathbf{x}_1, \dots, \mathbf{x}_N)$ corresponds to vector arrangements of possibly overlapping patches around pixels. We represent different features in data using (positive) representation functions:

$$f_d(\mathbf{x}_i), \quad (8)$$

so that the convolution operations over data become multiplications over representation functions. For the representation functions, index $d \in \{1, \dots, M\}$, where M is the number of different features in data that we wish to distinguish and can be combinatorially large with respect to the number of pixels.

For classification tasks, we view a neural network as a mapping from a particular instance to a cost function (e.g., the log probability) over labels y for that instance. With the new representation of data instances following Eq. (8), the mapping can be represented by a tensor \mathcal{A}^y operated on the combination of the representation functions:

$$h_y(\mathbf{x}_1, \dots, \mathbf{x}_N) = \sum_{d_1, \dots, d_N=1}^M \mathcal{A}_{d_1, \dots, d_N}^y \prod_{i=1}^N f_{d_i}(\mathbf{x}_i). \quad (9)$$

To be able to distinguish data instances \mathbf{x} from $\tilde{\mathbf{x}}$, we need $h_y(\mathbf{x}_1, \dots, \mathbf{x}_N) - h_y(\tilde{\mathbf{x}}_1, \dots, \tilde{\mathbf{x}}_N)$ to be nonzero. For a fixed mapping \mathcal{A}^y , this requirement is equivalent to:

$$\sum_{d_1, \dots, d_N=1}^M \mathcal{A}_{d_1, \dots, d_N}^y \left(\prod_{i=1}^N f_{d_i}(\mathbf{x}_i) - \prod_{i=1}^N f_{d_i}(\tilde{\mathbf{x}}_i) \right) \neq 0,$$

for $\mathbf{x} \neq \tilde{\mathbf{x}}$. It can directly be seen that the inequality is satisfied when the difference $\prod_{i=1}^N f_{d_i}(\mathbf{x}_i) - \prod_{i=1}^N f_{d_i}(\tilde{\mathbf{x}}_i)$ is not in the null space of $\mathcal{A}_{d_1, \dots, d_N}^y$. Therefore, the expressive power is equivalent to the *rank* of the tensor \mathcal{A}^y . This approach, taken by [5], establishes that for a certain type of networks, the rank of \mathcal{A}^y scales as n^{2^L} with measure 1 over the space of all possible network parameters, where n is the number of channels between network layers (width) and L is the network depth.

If we directly apply the theorem to a wider network (width m satisfying $m > n$), then the rank of \mathcal{A}^y will scale as m^{2^L} , which is $\left(\frac{m}{n}\right)^{2^L}$ times better. However, when the channels are gated with sparse weights, the set of \mathcal{A}^y with this restriction has measure 0 in the overall space of network parameters. In fact, if the number of nonzero weights over the channels is n , then the rank of \mathcal{A}^y still scales as n^{2^L} .

What makes our DeepMoE prevail is that (the sparsity pattern of) our mapping \mathcal{A}^y depends on the data. We hereby compare an L -layer DeepMoE with width equal to m and number of nonzero weights over the channels equal to $n < m$ against an L -layer fixed, non-sparse neural network with width equal to m . For the latter, we know that it will be able to distinguish between features in a subspace of dimension m^{2^L} . For the former, if $h_y(\mathbf{x}_1, \dots, \mathbf{x}_N) - h_y(\tilde{\mathbf{x}}_1, \dots, \tilde{\mathbf{x}}_N) \neq 0$ for the same choices of features (in the m^{2^L} dimensional subspace), then we know that it will have expressive

power of at least m^{2^L} :

$$\begin{aligned}
& h_y(\mathbf{x}_1, \dots, \mathbf{x}_N) - h_y(\tilde{\mathbf{x}}_1, \dots, \tilde{\mathbf{x}}_N) \\
&= \sum_{d_1, \dots, d_N=1}^M \mathcal{A}_{d_1, \dots, d_N}^y \prod_{i=1}^N f_{d_i}(\mathbf{x}_i) - \sum_{d_1, \dots, d_N=1}^M \tilde{\mathcal{A}}_{d_1, \dots, d_N}^y \prod_{i=1}^N f_{d_i}(\tilde{\mathbf{x}}_i) \\
&= \sum_{d_1, \dots, d_N=1}^M \mathcal{A}_{d_1, \dots, d_N}^y \left(\prod_{i=1}^N f_{d_i}(\mathbf{x}_i) - \prod_{i=1}^N f_{d_i}(\tilde{\mathbf{x}}_i) \right) \tag{10}
\end{aligned}$$

$$+ \sum_{d_1, \dots, d_N=1}^M \left(\mathcal{A}_{d_1, \dots, d_N}^y - \tilde{\mathcal{A}}_{d_1, \dots, d_N}^y \right) \prod_{i=1}^N f_{d_i}(\tilde{\mathbf{x}}_i). \tag{11}$$

Since the gating network is independent from the convolution neural network, to have Line (10) exactly equal to the negative of Line (11)—when they are both nonzero—has zero measure over the space of network parameters (even with the sparsity constraint). We simply need to focus on the cases where Line (10) is zero for the pair of \mathbf{x} and $\tilde{\mathbf{x}}$, and discuss whether Line (11) is also zero. In those cases, we assume that the sparsity pattern of the weights over the gated channels is i.i.d. with respect to each channel. With this assumption, probability of choosing exactly the same channels for different data: $\mathcal{A}_{d_1, \dots, d_N}^y = \tilde{\mathcal{A}}_{d_1, \dots, d_N}^y$ is $\binom{m}{n}^{-L}$. When they are not equal, the difference $\mathcal{A}_{d_1, \dots, d_N}^y - \tilde{\mathcal{A}}_{d_1, \dots, d_N}^y$ can be represented as combinations of linearly independent basis in \mathbb{R}^{M^N} and positivity of the representation functions ensures that Line (11) is not zero with probability 1. Therefore, $h_y(\mathbf{x}_1, \dots, \mathbf{x}_N) - h_y(\tilde{\mathbf{x}}_1, \dots, \tilde{\mathbf{x}}_N) \neq 0$ holds with probability $1 - \binom{m}{n}^{-L}$. In other words, there is a $1 - \binom{m}{n}^{-L}$ probability that the expressive power of our DeepMoE equals to or bigger than m^{2^L} .

A.2 Application on Semantic Segmentation

To evaluate the ability of DeepMoE to generalize to tasks beyond image classification, we conduct experiments of semantic segmentation which enables dense predictions over every pixel in the image on the Cityscapes dataset [8]. The Cityscapes dataset has 2975 training images, 500 validation images, and 1525 test images with 19 semantic categories. Each image in the dataset has a resolution of 2048×1024 . For data augmentation, we follow [26] to enable random cropping and basic mirroring and shifting augmentation.

We apply DeepMoE to DRN-A [26] and follow the training/testing procedure of [26] for fair comparison. We first pretrain DeepMoE on ImageNet and then finetune it on Cityscapes. The optimizer is SGD with momentum 0.9. The starting learning rate is set to $5e-4$ and divided by 10 after 200 epochs. The crop size is set to 832. We report the results in mean intersection-over-union (mIoU) score of wide-DeepMoE in Tab. 3.

By adjusting the hyper-parameter λ , we are able to obtain different accuracy-efficiency trade-offs which could either be more optimized for the computation efficiency or the prediction accuracy. Our efficient model wide-DeepMoE-50 v1 beats the baseline by 1.5% of mIoU with a slight increase in FLOPs, while our accurate model wide-DeepMoE-50 v2 outperforms the wide baseline by almost 2% of mIoU with lower FLOPs.

	Road	Sidewalk	Building	Wall	Fence	Pole	Light	Sign	Vegetation	Terrain	Sky	Person	Rider	Car	Truck	Bus	Train	Motorcycle	Bicycle	mean IoU	FLOPs($\times 10^6$)
DRN-A-50	96.9	77.4	90.3	35.8	42.8	59.0	66.8	74.5	91.6	57.0	93.4	78.7	55.3	92.1	43.2	59.5	36.2	52.0	75.2	67.3	703
wide-DeepMoE-50 v1	97.2	78.9	90.3	45.6	48.4	56.2	61.6	72.9	91.6	60.7	94.2	77.4	50.6	92.5	48.7	68.7	44.1	52.7	74.2	68.8	804
wide-DRN-A-50	97.4	80.6	90.6	38.5	49.0	58.7	65.1	73.4	91.8	59.5	93.9	78.2	51.1	92.9	49.1	68.7	51.3	52.2	74.5	69.3	2173
wide-DeepMoE-50 v2	97.5	80.4	91.0	48.9	50.6	58.5	65.7	75.3	92.0	60.1	94.7	79.2	54.7	93.2	53.8	73.2	53.2	54.8	75.6	71.2	1738

Table 3: Semantic Segmentation Results on Cityscapes

A.3 Gating Pattern Visualization

To analyze the gating behavior of DeepMoE, we visualize the gating pattern of DeepMoE with VGG-16 [22] as the base model on the CIFAR-100 dataset. The CIFAR-100 dataset has 100 fine-grained classes which can be grouped into 20 coarse categories. We evaluate the trained DeepMoE on the CIFAR-100 test set and save the gate outputs. We discretize the gate outputs to 0 and 1 (for all non-zero elements) which is a bitmap for each input image. We calculate the average value of the bitmaps of images in the same fine-grained classes and plot the heat-map for each class. In Fig. 7, we show the gating pattern of 5 fine-grained classes: *seal*, *beaver*, *whale*, *dolphin* and *otter* which belong to the same coarse class *aquatic mammals*. The gating patterns of *whale* and *dolphin* are pretty similar to each other while the other three classes share a similar pattern. If we look at the actual images of these classes, we can visually recognize that the whale and dolphin have similar appearance with smooth skin while the beaver and otter are more alike with dark fur. This indicates that the gate network is able to recognize the visual difference of the input images and select specialized expert combinations for that class.

Furthermore, we put additional visualization on the gate embedding shuffling experiments in sec. 5.3 in Fig. 8 which is equivalent to the bar chart in Fig. 6a.

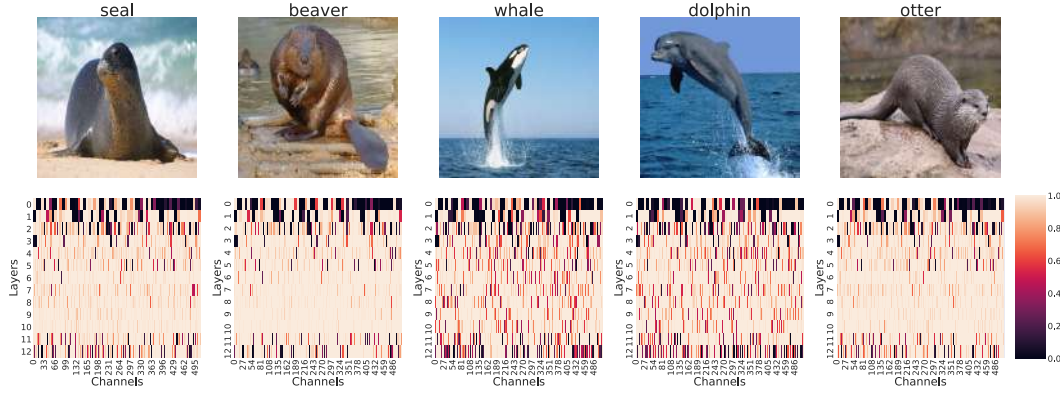


Figure 7: Visualization of the gating patterns on CIFAR-100

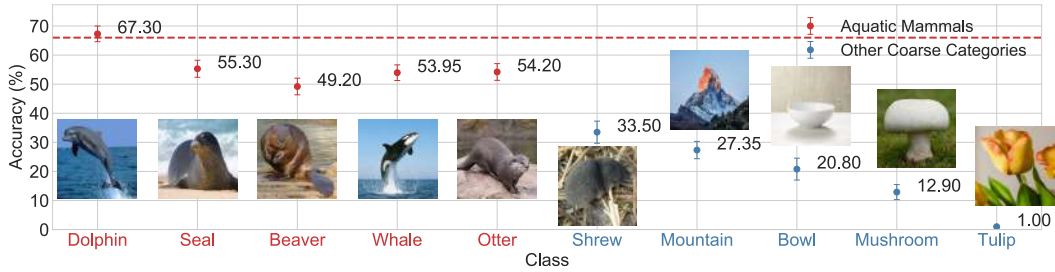


Figure 8: Gate embedding shuffling. The in-group shuffling has much higher accuracy than the out-of-group shuffling

A.4 Network Configurations of Wide VGG

In Sec. 5.4, we conduct experiments to investigate different widening strategies. We used four different strategies to widen the VGG-16 network which contains 13 convolutional layers in total: W1-High widens the top layer only, W1-Mid widens the middle layer only, W4-Low widens the lower 4 layers, and finally W13-All that widens all 13 convolutional layers in Tab. 4.

Layers	W1-High	W1-Mid	W4-Low	W13-All
Conv1	64	64	512	128
Conv2	64	64	512	128
Max Pooling	-	-	-	-
Conv3	128	128	615	256
Conv4	128	128	615	256
Max Pooling	-	-	-	-
Conv5	256	2990	256	405
Conv6	256	256	256	405
Conv7	256	256	256	405
Max Pooling	-	-	-	-
Conv8	512	512	512	615
Conv9	512	512	512	615
Conv10	512	512	512	615
Max Pooling	-	-	-	-
Conv11	1536	512	512	615
Conv12	512	512	512	615
Conv13	512	512	512	615
Max Pooling	-	-	-	-
Soft-max	-	-	-	-

Table 4: Channel configurations of different widening strategies